

## A computational tool for the design of ride control systems for fast planing vessels

A.A.K. Rijkens\*, J.A. Keuning and R.H.M. Huijsmans

*Ship Hydromechanics and Structures, Delft University of Technology, Delft, The Netherlands*

Received 23 September 2011

Accepted 2 November 2011

An effective method to reduce the violent motion behaviour of fast planing vessels in waves may be found in the application of active control devices in conjunction with advanced motion control systems. This study aims to develop a computational tool for the design and optimization of these ride control systems for high speed planing monohulls. Hydrodynamic characteristics of both transom flaps and interceptors are determined by systematic series of model test experiments in the towing tank of the Laboratory of Ship Hydromechanics at the Delft University of Technology. Transom flap results at downward deflection angles are validated with formulations found in literature. In addition, experiments at up angle flap positions have been performed to increase the range of application for motion control purposes. The hydrodynamic performance of the interceptors and transom flaps are compared in order to determine their efficiency. The experimental data was implemented in a nonlinear time domain mathematical model that can predict the seakeeping behaviour of fast monohulls. Simulations demonstrate the improvement in motion behaviour of a fast planing vessel with a ride control system sailing in head waves.

Keywords: Ride control systems, transom flaps, interceptors, planing vessels

### 1. Introduction

The continuous demand for planing monohulls that are able to operate in offshore conditions at high speeds results in the need to seriously improve their seakeeping performance. For many years, the design process was aimed to obtain the highest forward speed by reducing the resistance in calm water. As a consequence the earlier planing monohulls were known for their notorious bad seakeeping behaviour. In the last decades research projects focused more on improving the seakeeping characteristics. Changing hull shape design has significantly improved the behaviour of planing vessels in waves. However, the operational area of these ships is still limited to more or less sheltered areas and mild seas.

---

\*Corresponding author: A.A.K. Rijkens, Ship Hydromechanics and Structures, Delft University of Technology, Mekelweg 2, 2628 CD Delft, The Netherlands. E-mail: a.a.k.rijkenst@tudelft.nl.

Planing craft are nowadays widely used by various authorities in the role of patrol boats, Coast Guard vessels and search and rescue vessels. An important issue with these fast ships is their generally limited capability to remain fully operational at high forward speeds in relative large waves. The severe motions and in particular the occurrence of large vertical acceleration levels prevent the crew from fully utilizing the speed performance of the vessel. Voluntary speed reductions are often necessary to ensure a comfortable and safe ride or prevent constructional damage to the ship. The operational profiles of these vessels however, require high speed performance in offshore conditions.

Valuable research projects in the past contributed to the understanding and the origin of the violent motion behaviour of fast ships. Improving the seakeeping characteristics by changing hull form parameters meant one had to compromise on the calm water resistance performance. Increasing the deadrise angle resulted in a considerable gain in seakeeping ability at the cost of some power as was indicated by van den Bosch [18]. Fridsma [5,6] conducted an extensive systematic research on the seakeeping behaviour of planing models with constant deadrise angles in regular and later in irregular waves. He concluded that besides the deadrise angle, the dynamic (or running) trim is an equally important parameter for the behaviour in waves. So, hull form design as well as the actual position in the water at speed can significantly influence the seakeeping performance.

Ride control systems can be used to improve the motion behaviour of the vessel in waves by controlling its position at speed. Model tests experiments conducted by Wang [20] demonstrated the reduction in heave and pitch motions of a planing vessel equipped with active transom flaps. The deflection angle of the flaps was controlled proportional to the pitch velocity of the vessel. This control scheme proved to be very effective in reducing the motions of the model sailing in regular head waves. However, more advanced control systems need to be designed to minimize the motions of fast ships operating in various (irregular) wave conditions. An accurate simulation program that can predict the effects of active devices on the motion behaviour of fast ships is considered to be a valuable tool regarding the design of these complex control systems.

In this study a mathematical program that was originally used to predict the heave and pitch motions of planing vessels in waves, has been extended to consider the influence of active control devices. This computational program was firstly presented by Zarnick [22] and later further developed by Keuning [10]. Model test experiments have been conducted in the towing tank facility of the Laboratory of Ship Hydromechanics at the Delft University of Technology, to determine the hydrodynamic characteristics of transom flaps and interceptors in steady running conditions. The experimental work of Wang [20] is used to validate the present mathematical tool. Finally, simulations of a full scale vessel sailing in irregular waves are presented to illustrate the potential benefits of ride control systems to increase the operability of fast planing monohulls.

## 2. Ride control

Controlling the motions of a ship to improve its seakeeping behaviour has already been widely applied in the fast ferry market. Fin stabilizers are frequently installed on large ferries to control their roll motion behaviour. For reduction of the vertical motions in head waves control systems using trim flaps or T-foils or a combination of both can be rather effective, see for example Katayama, Suzuki and Ikeda [9] and Santos, Lopez and de la Cruz [13]. Controllability of a vessel, as defined by Calix St. Pierre et al. [3], is the ability to handle the vessel well within the limits of the desired behaviour. High speed ferries therefore often have multiple actuators to improve manoeuvring and seakeeping simultaneously. An extensive study to improve both passenger comfort and manoeuvring capabilities of a fast ferry using a ride control system is presented by van der Klugt, van Walree and Pauw [19]. Extensive model testing was carried out to determine a mathematical model of the vessel with all its control surfaces, see Jurgens et al. [8]. Later, Jurgens and van Walree [7] performed voyage simulations using the ferry with the ride control system and showed a significant reduction in the probability of exceeding certain Motion Sickness Incidence (MSI) threshold levels compared to the bare hull vessel.

These works demonstrate the possibilities of ride control systems to attenuate the motions of large high speed ferries (over 100 m). Smaller hard chine planing vessels (up to 30 m) have a more violent motion response in waves. These vessels generally operate in relatively large waves due to their limited overall dimensions. Furthermore, a substantial hydrodynamic lift is generated at high speeds that cause a considerable change in the sinkage and trim compared to the “reference position” at zero forward speed. The important effect of the running trim and sinkage on the motions and accelerations of a planing vessel sailing in waves was already indicated by Fridsma [5] and Keuning [10]. An increase of two degrees from  $4^\circ$  to  $6^\circ$  trim produced 50 to 100% higher values for the vertical accelerations both at the centre of gravity as well as at the bow. The relatively large wave exciting forces together with the nonlinear hydrodynamic lift on the hull results in a strong nonlinear motion response to incoming waves. Consequently, motions and especially maximum acceleration levels will be much higher compared to the large passenger ferries. This nonlinear motion behaviour makes the design for an effective ride control system a rather challenging job.

### 2.1. Trim control of planing vessels

Controlling the running trim and consequently the sinkage, as these two are closely related to each other, appeared to be important optimization parameters for planing vessels. Similar to research studies on planing hull form design, earlier works concentrated on the effectiveness of wedges or flaps on the smooth water performance. Millward [12] investigated the effect of a trim wedge to lower the overall resistance of planing hulls. He suggested that wedges (or flaps) have a dual effect, in addition

to the apparent effect of altering the trim of the vessel, the wedges will also increase the hydrodynamic lift on the hull. The effect of the wedge on the hydrodynamic lift causes a change in resistance other than that would be obtained by a longitudinal movement of the centre of gravity. The optimum trim angle for a given hull shape at fixed displacement changes with forward speed. For overall performance it is therefore necessary to use a flap with an adjustable angle.

Another calm water application for trim control was found in the correction of dynamic instability problems. High speed planing vessels can suffer from undesirable oscillatory motions without any apparent excitation from the environment. These problems are caused by the complicated nature of the hydrodynamic lift acting on the hull. Instabilities can manifest in either longitudinal or transverse directions or a combination of both. A worthwhile overview of dynamic instabilities of high speed planing boats is given by Blount and Codega [1]. One of the most well-known instability phenomena is the combined oscillatory motion in both pitch and heave, referred as porpoising. Savitsky [14] concluded that a wedge could be used to lower the running trim which may in general postpone porpoising inception, however this could lead to unfavourable low trim angles. More recently, Xi and Sun [21] used a controllable transom flap with feedback control to successfully eliminate porpoising for a planing vessel.

### 2.2. Motion control of planing vessels in waves

Active control devices like, transom flaps or interceptors (Fig. 1) can generate large dynamic forces at high speeds which will increase the controllability of the vessel in waves. These systems are primarily used for the reduction in pitch and heave [20], however roll and even yaw motions can also be influenced if port and starboard sides of the mechanisms are independently operated. This study only considers motion control systems governing the pitch and heave motions of planing vessels operating in head waves.

## 3. Hydrodynamic characteristics of the control devices

The hydrodynamic characteristics of the control devices will be implemented into a mathematical model to enable the design of motion control systems in a software

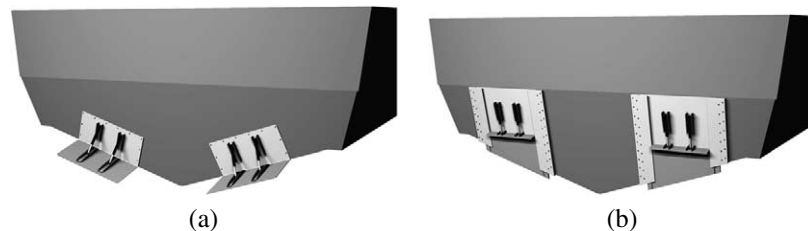


Fig. 1. Active control devices. (a) Active transom flaps. (b) Active interceptors.

environment. This requires an accurate prediction of the hydrodynamic forces added by the control surfaces. In this study a comparison is made between the hydrodynamic characteristics of transom flaps and interceptors.

### 3.1. Transom flaps

Brown [2] conducted a systematic study on the effects of transom flaps on planing hulls. The goal of this study was to provide the designer expressions for controlling the running trim. The results could be easily incorporated into the existing sets of planing formulae derived by Savitsky [14]. The lift generated with a flap is a function of the flap area and the deflection angle. Besides the lift resulting from the pressure increase on the flap surface itself, a considerable fraction of the lift is produced by the modified pressure distribution under the hull surface extending forward of the transom (Fig. 2(a)). The lift increment coefficient due to flap deflection was defined by Brown [2] as:

$$\Delta C_{L_f} = 0.046\lambda_f\sigma\alpha_f. \tag{1}$$

Next to the induced drag, which is increased by increasing flap deflections, an additional increase in the pressure on the flap itself is present.

$$\Delta C_{D_f} = 0.00024\lambda_f\sigma\alpha_f(\tau + \alpha_f), \tag{2}$$

in which:  $\lambda_f$  – flap chord-beam ratio;  $\sigma$  – flap span-beam ratio;  $\alpha$  – deflection angle of the flap;  $\tau$  – trim angle.

The definition of the added forces of the flaps is presented in Fig. 3. The longitudinal distance of the added lift is normalized with respect to the beam of the model. Brown [2] found that the location of the centre of pressure of the flaps measures 0.6 times the beam ahead of its trailing edge, regardless of flap area or deflection

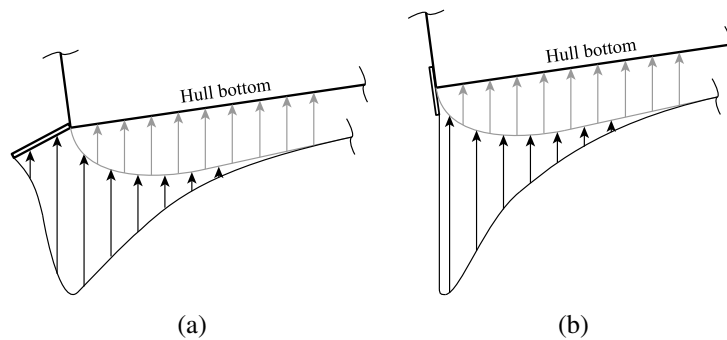


Fig. 2. Schematic pressure distribution bare hull (grey) and added pressure distribution due to control devices (black). (a) Pressure distribution flap. (b) Pressure distribution interceptor.

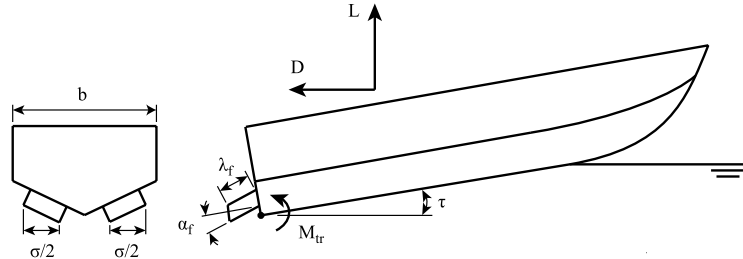


Fig. 3. Definition of forces.

angle. Thus, the moment increment coefficient of the flap about the transom-keel intersection becomes:

$$\Delta C_{M_{tr,f}} = \Delta C_{L_f}(0.6 - \lambda_f). \quad (3)$$

Later, Savitsky and Brown [16] refined this equation to better account for partial-beam flaps. The distance of the added lift for partial-beam flaps acts  $0.6 + \lambda_f(1 - \sigma)$  times the beam ahead of the trailing edge of the flaps. The moment increment coefficient for these partial-beam flaps about the transom-keel intersection corresponds to:

$$\Delta C_{M_{tr,f}} = \Delta C_{L_f}(0.6 - \lambda_f\sigma). \quad (4)$$

Note that for full-span flaps where  $\sigma = 1$ , this equation reduces to Eq. (3).

These formulae are valid for downward flap deflections, ranging from  $0^\circ$  to  $15^\circ$ . A wide range of flap angles will increase the controllability of the vessel. It would therefore be interesting to investigate if flaps can produce negative lift forces, resulting in a bow-up trimming moment. To generate these forces the flaps need to be at an up angle position. However, the water will detach from the surface of the flap if the angle exceeds a certain limit. At this instant the lift produced by the flap will drop significantly. Model experiments will be carried out to determine at what deflection angle the flow starts to separate.

### 3.2. Interceptors

Interceptors are nominal vertical plates mounted on the transom surface of a vessel. The bottom sides of these plates generally follow the shape of the transom edge. Active control systems can lower the interceptors into the flow stream which increases the immersed area. The protruding blades cause a stagnation flow region which modifies the surrounding flow over a certain distance underneath the hull. This stagnation region is characterized by a high pressure and induces a lift force on the stern of the vessel. In contrast to the transom flap no lift force will be acting upon

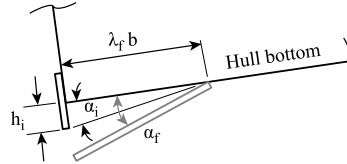


Fig. 4. Geometrical interceptor angle (black) and corresponding flap angle (grey).

the interceptor itself, the increase in lift is entirely the result of the change in pressure distribution underneath the hull (Fig. 2(b)). A variation in lift can be obtained by altering the height of the interceptors.

Dawson and Blount [4] suggested formula that relates a particular flap angle to an interceptor excursion that produces an equivalent lift force (Fig. 4). Assuming that the interceptor and the flap have the same span, the relation between the flap angle  $\alpha_f$  and the geometrical interceptor angle  $\alpha_i$  can be approximated by:

$$\alpha_i = 0.175\alpha_f + 0.0154\alpha_f^2. \quad (5)$$

The flap angle  $\alpha_f$  may not exceed the  $15^\circ$ , which corresponds to a maximum geometrical interceptor angle  $\alpha_i$  of approximately  $6^\circ$ . The excursion of the interceptor can subsequently be derived using the defined chord length of the corresponding transom flap:

$$h_i = \lambda_f b \sin \alpha_i. \quad (6)$$

In the recovered position no lift force is generated, after all the blades are completely hoisted out of the transom flow stream. This also means that it is not possible to generate negative lift forces resulting in a bow-up trimming moment with these devices. To determine the efficiency of the interceptors, both the added lift and drag forces will be measured in the model experiments. The moments on the model will be measured to derive the longitudinal position of the centre of pressure of the added lift.

### 3.3. Experimental setup and procedure

A systematic series of captive model tests have been carried out in the towing tank of the Laboratory for Ship Hydromechanics at the Delft University of Technology, in order to determine the hydrodynamic characteristics of the transom flaps and interceptors. A V-shaped prismatic model is used which is divided into two segments. The front segment has a length of 1.6 m and the aft segment is 0.4 m long. The overall beam measures 0.4 m and the model has a constant deadrise angle of  $20^\circ$ . These two segments are connected with a horizontal girder located above the model.

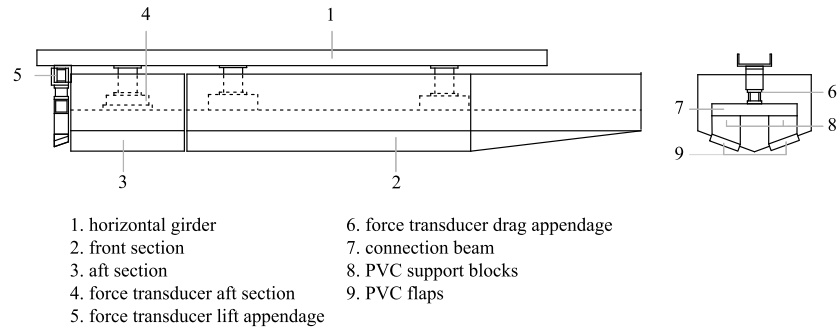


Fig. 5. Schematic representation model.

An additional support frame was connected to the girder for testing flaps and interceptors. This frame is designed to easily change different flap angles and interceptor excursions during the experiments. The flaps itself were made of PVC blocks with the lower surface machined to the required flap angle to ensure its being accurately maintained. The interceptors were constructed out of angle sections that could also be fitted on the support frame. The flaps and interceptors had span of  $\sigma = 0.6$  and the chord length of the flaps measured  $\lambda_f = 0.125$ . A schematic representation of the model can be seen in Fig. 5.

The forces on the model and on the flaps were measured separately to qualify the interaction effects of the flaps on the model. The contribution of the added forces due to the deflection of the control devices are expected to be small with respect to the total force on the model itself. The added forces of the flaps or interceptors are therefore measured on the aft segment of the model, which may improve the level of accuracy of the measurements. The spacing between the segments is kept to a minimum within the working precision of the equipment available and had a value of approximately 1 mm. However, to avoid disturbances in the flow stream a latex strip was used to close the spacing. The latex strip had a thickness of only 0.4 mm to prevent cross talk of forces between the segments.

The model was connected to a hydraulic oscillator based on a Stewart platform. This device can easily position the model to test different trim angles. The prescribed position was measured by a camera system tracking LEDs on the model. All data acquisition systems as well as the equipment to drive and control the oscillator were installed on the towing carriage. On the bottom of the tank an underwater camera was installed to photograph the wetted surface of model at speed. These photos will be used to determine the wetted length of the model and check for possible disturbances in the flow. To measure the forces in the aft segment a 6-component force transducer was installed. The lift and drag on the trim device were measured with two ordinary strain gauge type force transducers.

The model was tested in three configurations: the reference bare hull model, the model with transom flaps and the model with interceptors. The independent variables that were investigated during the experiments are listed in Table 1.

Table 1  
Tested variables

Variable	Symbol	Values	Unit
Speed	$V$	3.0, 4.0, 5.0, 6.0	m/s
Trim angle	$\tau$	2, 4, 6, 8	deg
Flap angle	$\alpha_f$	-8, -4, 0, 8, 16	deg
Interceptor excursion	$h_i$	7, 14	mm

### 3.4. Results transom flaps

The mean wetted length of a planing vessel is a fundamental quantity in the planing analysis used in the formulations derived by Savitsky [14]. By adding transom flaps this wetted length will be increased. According to Brown, the mean wetted length of a planing vessel with flaps can be determined using Eq. (7), where the average of the keel and chine lengths are taken plus an allowance for the stagnation line curvature and the contribution of the surface of the flaps.

$$\lambda_m = 0.5(\lambda_k + \lambda_c) + 0.03 + \lambda_f \sigma, \quad (7)$$

in which:  $\lambda_m$  – mean wetted length-beam ratio;  $\lambda_k$  – keel wetted length-beam ratio;  $\lambda_c$  – chine wetted length-beam ratio;  $\lambda_f$  – flap chord-beam ratio;  $\sigma$  – flap span-beam ratio.

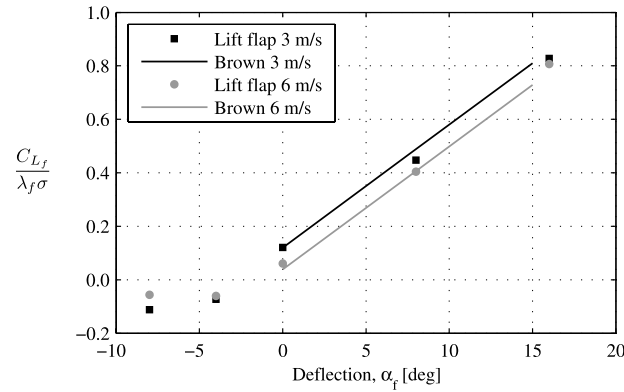
The wetted lengths were determined based upon the underwater photos taken during the experiments. The lift of the planing surface, both with and without flaps can subsequently be calculated using Eq. (8) [2].

$$\begin{aligned} C_{L_{b,f}} &= 0.25\pi \sin 2\tau \cos \tau \\ &\times \left[ \frac{(1 - \sin \beta)\lambda_m}{1 + \lambda_m} + \frac{C_{D,c}}{\pi} \lambda_m \sin 2\tau \cos \beta + \frac{0.4}{\cos \tau} \left( \frac{\lambda_m}{C_V} \right)^2 \right] \\ &+ \Delta C_{L_f}. \end{aligned} \quad (8)$$

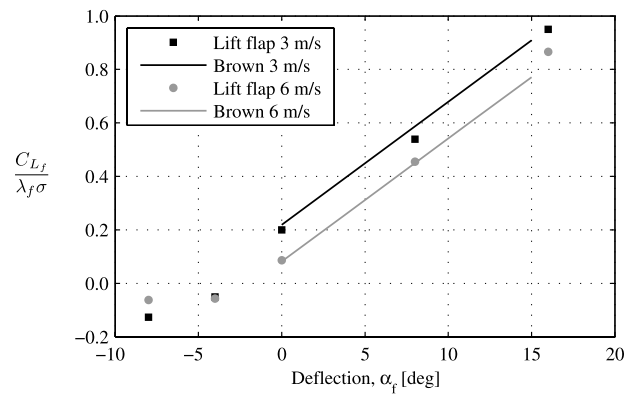
The lift generated by the transom flaps can now be obtained by subtracting the calculated bare hull lift from the calculated lift of the model with the transom flaps.

$$C_{L_f} = C_{L_{b,f}} - C_{L_b}. \quad (9)$$

The calculated results are compared with the experimental results in Fig. 6. The two graphs illustrate the relation between the non-dimensional lift of the flap as function of its deflection angle. A selection in trim angles ( $4^\circ$  and  $8^\circ$ ) and velocities (3 and 6 m/s) are presented. The calculated values are in close agreement with the measured results. The lift coefficient is only slightly dependent on the trim of the model, where the differences are mainly caused due to an offset in the lift at zero



(a)



(b)

Fig. 6. Lift prediction Brown [2] (lines) and lift measurements flap (markers). (a) Lift coefficient flap – trim 4. (b) Lift coefficient flap – trim 8.

deflection angle of the flap. The lift slope is hardly influenced by a change in trim. A lower model speed results in higher values of the lift coefficient. This velocity dependence becomes bigger for larger trim angles and could possibly be explained by differences in the transom flow at various speeds.

Flaps can generate small negative forces at certain up angle positions. The linear range between flap angle and lift coefficient is however limited due to flow separation for larger up angle positions. Up to  $-4^\circ$  the linear trend holds, although small effects of flow separation were already noticed during experiments at higher velocities. At flap angles of  $-8^\circ$  the flow separation became more severe. The effect of this flow separation on the lift force is clearly visible in the results.

In Eq. (10) Brown [2] derived the drag of a planing surface using the lift plus a contribution due to viscous shear stresses acting parallel to the surface. An increase

in lift force on the planing surface as a result of flap deflection will consequently also increase the induced drag. The lengthening of the mean wetted length due to the wetted area of the flaps increases the viscous shear stresses. Finally, the extra pressure component on the flaps itself further augments the total drag of the model with transom flaps.

$$C_{D_{b,f}} = C_{L_{b,f}} \tan \tau + \frac{C_f \lambda_m}{\cos \tau} \cos \beta + \Delta C_{D_f}. \quad (10)$$

Subtracting the calculated bare hull drag from the calculated drag of the model with flaps, yields the total drag added by the transom flaps.

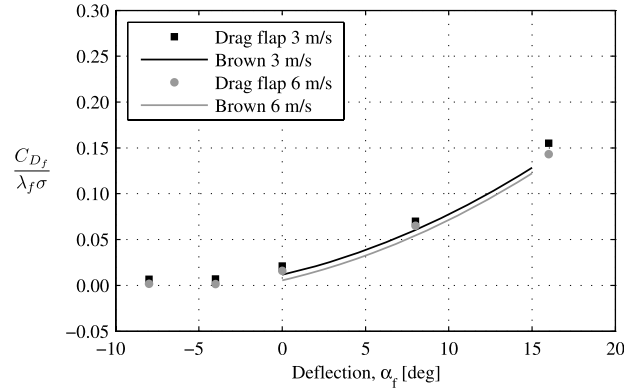
$$C_{D_f} = C_{D_{b,f}} - C_{D_b}. \quad (11)$$

The experimental results indicate a slightly larger drag compared to the calculated values as is shown in Fig. 7. This is probably due to the small spacing between the transom and the flaps. During the experiments a small amount of spray was noticed. However, the consistency in trends between the calculations and measurements is evident and differences are within the accepted level of tolerance. At downward flap angles the drag is very small and can almost be neglected.

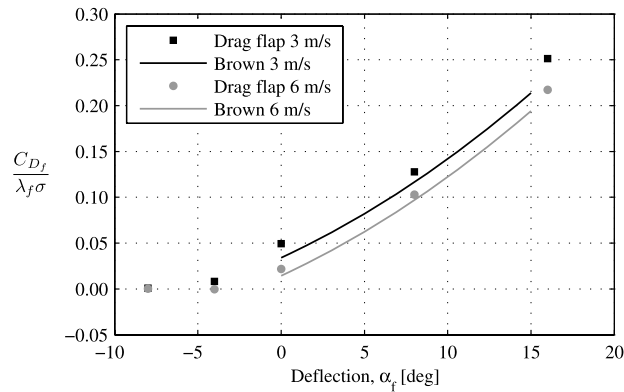
The pitching moment of the planing surface with flaps is defined by Brown [2] about a point on the keel line at a distance of  $\lambda_f \sigma$  aft of the transom. Consequently, if no transom flaps are installed i.e.,  $\lambda_f$  and  $\sigma$  are zero – the pitching moment is taken about the transom-keel intersection. The total pitching moment on the planing surface is given in Eq. (12) [2]:

$$\begin{aligned} C_{M_{b,f}} = & 0.25\pi \sin 2\tau \\ & \times \left[ \left( 0.875\lambda_m - 0.08 \frac{\tan \beta}{\tan \lambda_m} \right) \frac{1 - \sin \beta}{1 + \lambda_m} \right. \\ & \left. + \frac{C_{D,c}}{2\pi} \lambda_m \sin 2\tau \cos \beta + \frac{0.133}{\cos \tau} \left( \frac{\lambda_m}{C_V} \right)^2 \right] + \Delta C_{M_f}. \end{aligned} \quad (12)$$

In this article the pitching moment is defined about a fixed point on the transom-keel intersection. The moment coefficient calculated with Eq. (12) ( $C_M$ ) for the planing surface with flaps is therefore rewritten to a moment coefficient about the transom-keel intersection ( $C_{M_{tr}}$ ). The longitudinal position of the centre of pressure is normalized with the beam of the model and is measured from the transom edge forward. Brown found that the centre of pressure of the added lift is located at a distance of  $0.6 - \lambda_f \sigma$  times the beam ahead of the transom-keel intersection. However, the present experimental results indicate that the centre of pressure is located much more aft. Based upon the measurements it was found that the added lift of the flap



(a)



(b)

Fig. 7. Drag prediction Brown [2] (lines) and drag measurements flap (markers). (a) Drag coefficient flap – trim 4. (b) Drag coefficient flap – trim 8.

has a constant value of only  $0.25 - \lambda_f \sigma$  times the beam ahead of the transom edge. The moment increment coefficient about the transom-keel intersection denotes:

$$\Delta C_{M_{tr,f}} = \Delta C_{L_f} (0.25 - \lambda_f \sigma). \quad (13)$$

Unfortunately, no satisfactory explanation for this remarkable difference in longitudinal position of the centre of pressure has been found. It is assumed that the centre of pressure on the surface of the flaps is located at one third of the chord length aft of the transom edge. The lift ratio between the flap surface and the hull bottom area was found to be independent of speed, trim and deflection angle. One third of the added lift was generated by flap surface and the remaining two thirds was produced by the pressure change on the hull bottom area. The centre of pressure of the added lift on

the hull area was measured  $0.35 - \lambda_f \sigma$  times the beam ahead of the transom edge, corresponding to roughly two times the chord length of the flap. Given the distribution of the added lift between the flap surface and the hull bottom area, a total centre of pressure of  $0.25 - \lambda_f \sigma$  times the beam ahead of the transom edge is plausible.

The total added pitching moment can be calculated by subtracting the pitching moment of the bare hull from the pitching moment of the hull including flaps. In Eq. (14) the moment increment coefficient defined in Eq. (13) has been used.

$$C_{M_{tr,f}} = C_{M_{tr,b,f}} - C_{M_{tr,b}}. \quad (14)$$

The experimental results of the moment coefficient relative to the transom-keel intersection, together with Eq. (14) are shown in Fig. 8.

### 3.5. Results interceptors

The experimental results of the interceptors are given in similar graphs as the ones used to present the results of the transom flaps. The same reference area is used to make the forces and moments non-dimensional. The lift and drag are plotted versus the geometrical interceptor angle, which enables easy comparison with the transom flaps results.

In Fig. 9 the measured lift forces of the interceptors are presented, together with the formulation suggested by Dawson and Blount [4]. The interceptor excursions in the experiments were chosen such that the position of its lower edge equalled the deflection height of the trailing edge of the transom flaps. However, these interceptor excursions exceed the range of application of the formulation given by Dawson and Blount [4] (Fig. 9). For a better comparison experiments should be carried out with smaller interceptor excursions. The velocity dependence of the interceptors seems to be less compared to the transom flaps results. The flaps extend aft of the transom and differences in the transom flow shape at various speeds of the model, may lead to a small change in the pressure distribution on the surface of the flaps. Interceptors, are virtually located at the transom and no lift is generated on the blade itself. A change in transom flow shape at different model speeds may therefore have less influence on the lift coefficient.

Similar to the transom flaps, the drag coefficient for the interceptors is strongly dependent on the trim angle of the model. The relation between the drag coefficient and the geometrical interceptor angle is close to linear as indicated in Fig. 10. The longitudinal position of the centre of pressure of the added lift of the interceptor acts on a fixed point forward of the transom, see Fig. 11. The moment coefficient can be described using Eq. (15).

$$C_{M_{tr,i}} = 0.26C_{L_i}. \quad (15)$$

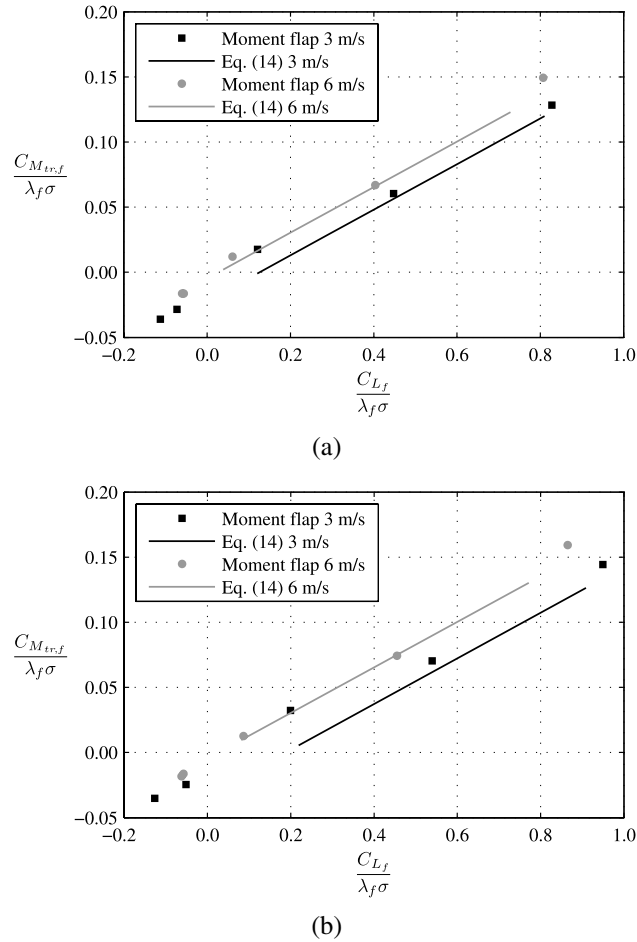
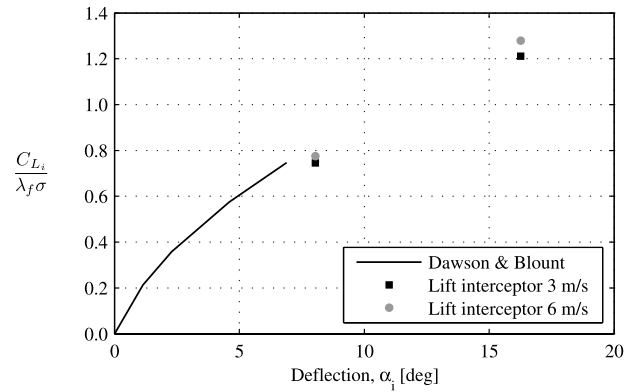


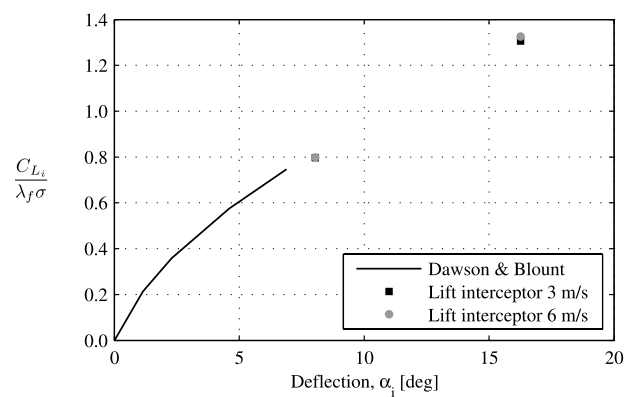
Fig. 8. Pitching moment Eq. (14) (lines) and pitching moment measurements flap (markers). (a) Moment coefficient flap – trim 4. (b) Moment coefficient flap – trim 8.

### 3.6. Efficiency of transom flaps versus interceptors

A higher or more favourable lift-to-drag ratio is typically one of the major goals in the design for control devices, since this will result in a maximum lift force at the expense of a minimal resistance penalty. To compare the efficiency of both trim devices the lift-to-drag ratios are visualized in Fig. 12. Trend lines are added for easy comparison, for the construction of these lines only the values for positive flap angles are considered. These lines suggest that there is no discernible difference between the efficiency of the transom flaps and the interceptors.



(a)

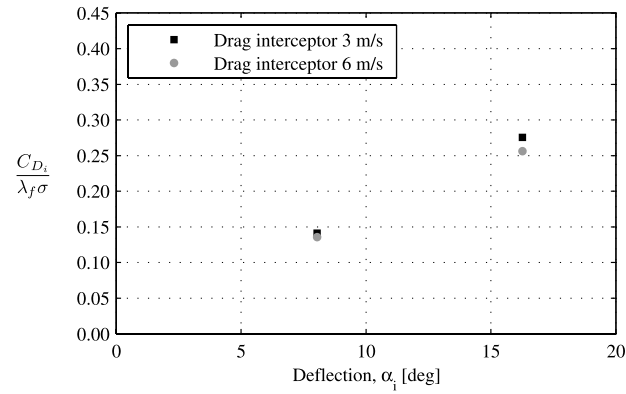


(b)

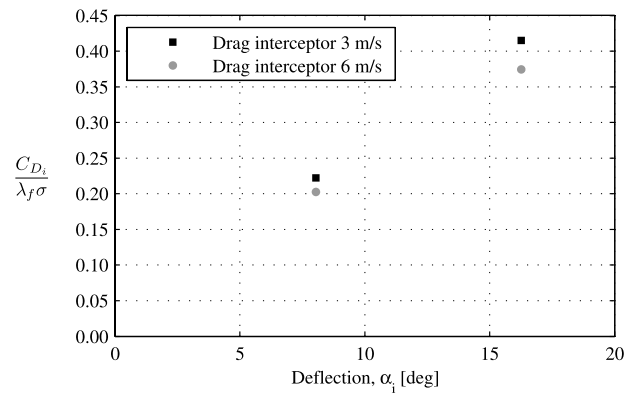
Fig. 9. Lift prediction Dawson and Blount [4] (line) and lift measurements interceptor (markers). (a) Lift coefficient interceptor – trim 4. (b) Lift coefficient interceptor – trim 8.

#### 4. The mathematical model

A mathematical model, that is able to predict the complex motion behaviour of a planing vessel sailing in waves, has been extended with empirical relations of the hydrodynamic characteristics of the control devices. The original mathematical program was firstly presented by Zarnick [22] and is later further developed and improved by Keuning [10]. This nonlinear time domain model can be used for the simulation of pitch and heave motions of a planing vessel sailing in irregular head waves. One of the great advantages of this model is the short computational time. In addition, the effects of the trim devices can easily be added to the equations of motion.



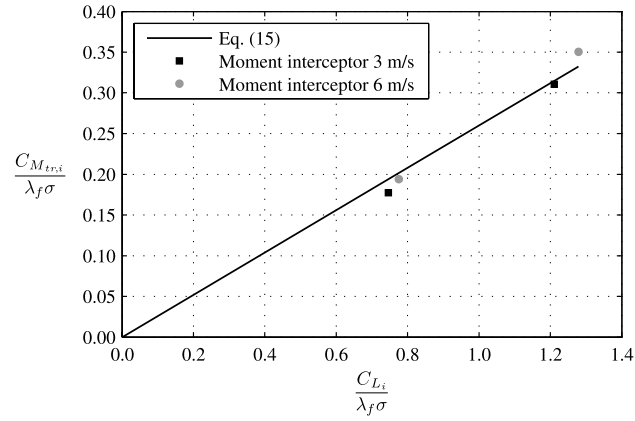
(a)



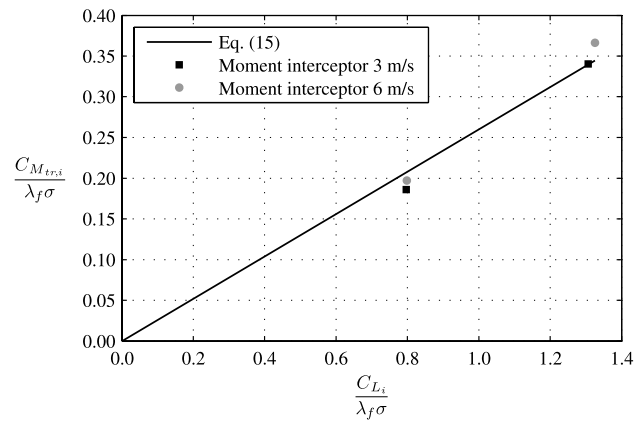
(b)

Fig. 10. Drag measurements interceptor (markers). (a) Drag coefficient interceptor – trim 4. (b) Drag coefficient interceptor – trim 8.

A brief description of the mathematical model is given which in particular focuses on the implementation of the hydrodynamic forces of the control devices. A complete explanation of both the theoretical background and the set of formulations of the forces involved may be found in the references [10,22]. The forces on the hull are determined based on a strip theory approach where the hull is divided in an arbitrary number of transverse sections. For each of these sections along the length of the hull the total force can be determined. These sectional forces constitute of a buoyancy force related to the momentary displaced volume, a hydrodynamic force component associated with the change of fluid momentum and a viscous contribution due to cross flow drag. Subsequently, total hydrodynamic forces acting on the vessel are obtained by integration of the sectional forces along the length of the hull.



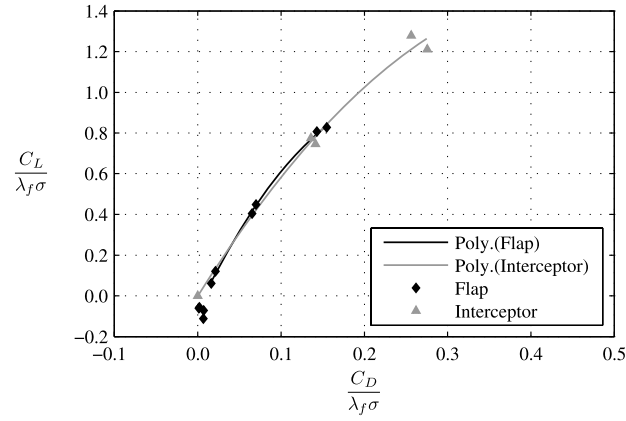
(a)



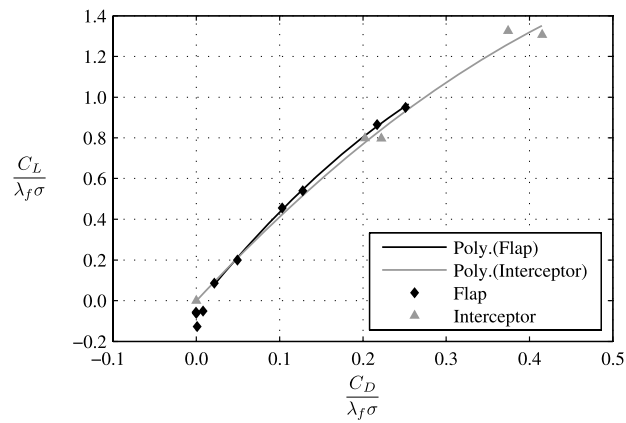
(b)

Fig. 11. Pitching moment Eq. (15) (line) and pitching moment measurements interceptor (markers). (a) Moment coefficient interceptor – trim 4. (b) Moment coefficient interceptor – trim 8.

Only motions in the vertical plane are considered and the perturbation in velocity is assumed to be small in comparison with the forward speed of the vessel. In addition, it is supposed that the working line of the frictional resistance and thrust force go through the centre of gravity and that the vertical components of these forces are small relative to other hydrodynamic forces involved and may therefore be neglected. The added forces generated by the trim device are based on the experimental values presented in this article. The instantaneous lift of the control devices at every time step is assumed to be equivalent to those for steady motion at corresponding deflection and trim angle, following the quasi-steady flow approximation. With these



(a)



(b)

Fig. 12. Lift-to-drag ratio of flap and interceptor. (a) Lift-to-drag ratio – trim 4. (b) Lift-to-drag ratio – trim 8.

simplifications taken into consideration, the equations of motion may be written:

$$\begin{aligned}
 M\ddot{x}_{CG} &= 0, \\
 M\ddot{z}_{CG} &= -N \cos \theta + W - L, \\
 I\ddot{\theta} &= Nx_N + Lx_L,
 \end{aligned} \tag{16}$$

in which:  $N$  – normal force;  $W$  – weight of the ship;  $L$  – lift of trim device;  $x_N$  – distance of the normal force relative to CG;  $x_L$  – distance of the added lift of the trim device relative to CG;  $\theta$  – pitch angle, see Fig. 13.

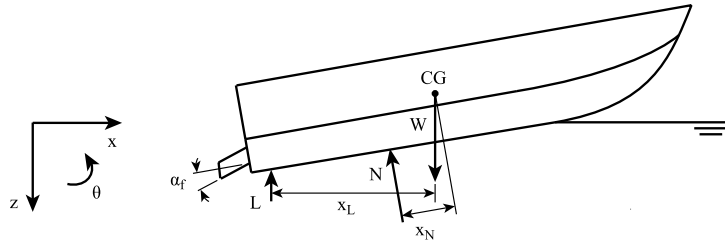


Fig. 13. Definition of forces in the mathematical model.

These equations of motion can be solved by the program in a time domain solution using standard numerical techniques.

#### 4.1. Control system

The control system basically regulates the behaviour of the actuators in order to minimize the motions of the vessel. It generally contains a control algorithm to process the real-time motions of the vessel to an output signal which actuates the control devices. In this study only the heave and pitch motions are considered. The deflection of the trim devices can therefore be based on any combination of these motions.

$$\alpha = \alpha_{heave}(z, \dot{z}, \ddot{z}) + \alpha_{pitch}(\theta, \dot{\theta}, \ddot{\theta}). \quad (17)$$

Complex control algorithms can be developed which may effectively reduce the motions of the vessel. However, to validate the mathematical model the same control law is used as has been applied by Wang [20] in his model experiments. Wang concluded that the heave motion is not so sensitive to the excitation force of flaps, which is small in comparison to the total hydrodynamic force on the hull. Furthermore, the registration of the real-time heave motions on board a vessel out on full seas encounters some practical concerns. The angle of the flap is therefore simplified as a function of the pitch motion only:

$$\alpha_f = K_\theta \theta + K_{\dot{\theta}} \dot{\theta} + K_{\ddot{\theta}} \ddot{\theta}, \quad (18)$$

where the  $K$  values represent the system gain coefficients. The pitch angle, pitch velocity and pitch acceleration may be used to increase the pitch restoring moment, damping and inertia of the vessel, respectively. Closer inspection of each of these signals individually revealed that the pitch velocity may be regarded as the best control parameter [20]. The pitch velocity may be considered to be the out of phase component with respect to the pitch angle of the vessel. A feedback system based on the pitch angle only was found to be rather ineffective, it even amplified motions and accelerations at certain intermediate wave frequencies. The strong nonlinear character of the pitch accelerations makes it less suitable for an input signal of the control

system. The deflection of the control devices based on a pitch velocity feedback becomes:

$$\alpha_f = K_{\dot{\theta}} \dot{\theta}. \quad (19)$$

The angle of the flap is limited to a minimum value of  $-4^\circ$  and a maximum angle of  $16^\circ$ . In addition, the maximum angular velocity of the flaps is restricted to  $\pm 40^\circ/\text{s}$ . The lift is assumed to be instantaneous relative the deflection angle of the flaps, i.e., no phase difference is taken into account. During the simulation it is assumed that the control devices remain fully submerged. In reality this may not always be the case if ship motions are large as for a sequence when the hull leaves or is close to leaving the water.

## 5. Simulations

### 5.1. Comparison between simulations and model test data in regular waves

Wang [20] used a planing vessel, referred as model 85, in regular waves with active transom flaps. This model was originally used by van den Bosch [18] to investigate the nonlinear response of a planing hull. The flaps spanned the complete transom and its chord length measured 0.125 times the beam of the model. The flaps had an initial deflection angle of  $4^\circ$ . The model tests were run at 4.5 m/s in regular waves ranging between 1 and 6 times the hull length and a wave height of 0.055 times the beam. The model was fitted with a rate gyro which recorded the pitch velocity. This signal was amplified to a suitable level and fed back to a shaker, which controlled the instantaneous angle of the flaps.

The gain coefficient  $K_{\dot{\theta}}$  can be changed to modify the magnitude of the response amplitude of the flap. Wang used a particular coefficient to express the relation between the flap excitation force and the pitch velocity. This coefficient was dependent on specific flap geometrical properties and the behaviour of the control system. In Figs 14 and 15 the original gain coefficient used by Wang has been converted to comply with the current definition for the pitch velocity gain coefficient  $K_{\dot{\theta}}$ . Several different values for the gain coefficients were used ranging from 0 to 0.8. For  $K_{\dot{\theta}} = 0$  the system is without feedback control and the position of the flap is always at its initial  $4^\circ$  deflection angle.

The calculated pitch response corresponds well with measurements of Wang, indicated in Fig. 14. Both the experiments as the simulations show a maximum pitch reduction in the amplitude response of about 60% near the resonant wave encounter frequency for the highest gain coefficient. The pitch response is improved over almost the complete wavelength region and for higher gain coefficients a stronger reduction in pitch response is noticed.

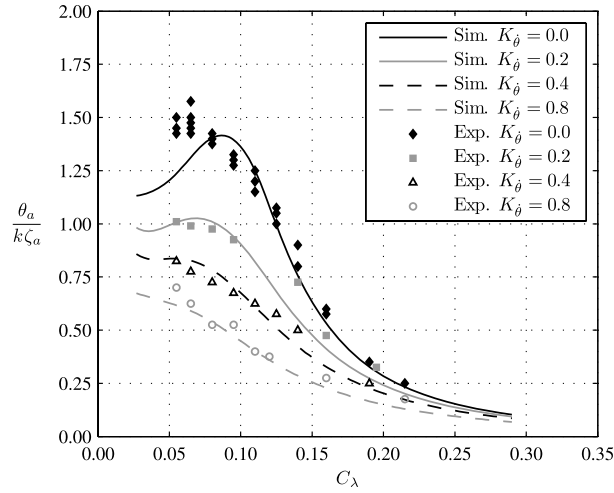


Fig. 14. Experimental [20] and calculated pitch response for model 85 at 4.5 m/s.

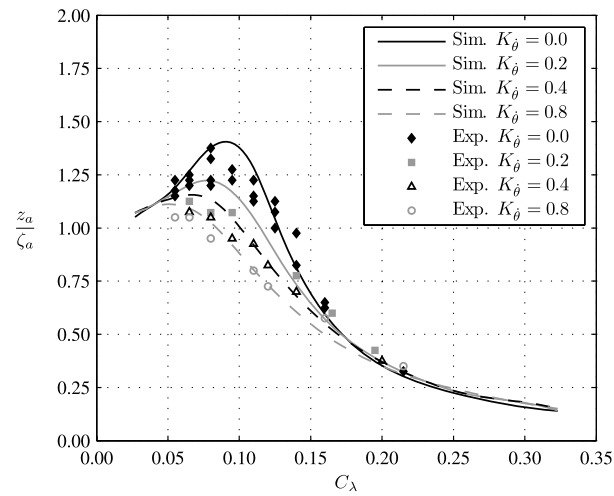


Fig. 15. Experimental [20] and calculated heave response for model 85 at 4.5 m/s.

The correlation between the measured and calculated results for the heave response in Fig. 15 deviates slightly near the resonance encounter frequency. Although, simulations do not agree over the complete range of wave lengths, the trend is considered to be predicted reasonably well. Pitch velocity feedback control has a positive effect on the reduction of the heave motion response of the vessel, as indicated by both experiments and simulations.

More recently, Savitsky [15] reports about model tests conducted at the Davidson Laboratory with a planing vessel using active transom flaps to improve its seakeeping behaviour. The experiments were quite similar to the ones carried out by Wang [20] and Savitsky found corresponding results. For a gain coefficient of  $K_{\dot{\theta}} = 0.56$  a reduction of 50% in the pitch motion amplitude response was achieved and the heave motion amplitude was nearly 30% reduced at the resonant condition. Next to the motions, accelerations at the centre of gravity have also been measured and a reduction of approximately 35% at the resonant frequency was found. Both studies indicate the potential benefits of active flaps to improve the motion behaviour of planing vessels. In addition, a lower resistance in waves was measured with the control system activated.

### 5.2. Full scale simulations in irregular waves using the ride control system

The motion reduction in regular waves near the resonant frequency is quite strong using a pitch velocity control scheme. As for most systems increasing the damping will result in a significant motion amplitude reduction, particularly near the resonance region. For irregular waves the excitation frequency varies and will consequently not necessarily be at this resonance condition. To examine the effect of the control system in irregular waves simulations have been carried out using the mathematical model.

In these simulations the waves are represented by a JONSWAP spectrum with a significant wave height of 1.25 m and a peak period of 6.5 s. A parent hull form of the Delft Systematic Deadrise Series (DSDS) with a deadrise angle of  $25^\circ$  is used in the simulations, which is scaled to a 15 m long planing vessel (Fig. 16). Two transom flaps are modelled measuring  $0.78 \times 0.29$  m each, corresponding to a total span of  $\sigma = 0.6$  and a chord length of  $\lambda_f = 0.125$ . These flaps are controlled with a pitch velocity feedback system using a gain coefficient of  $K_{\dot{\theta}} = 2.0$ . The forward speed of the vessels is 25 knots and the total simulation time equals 1 h. The relatively harsh operational conditions have been selected to provoke the extremes in vertical accelerations.

The time series of the first 30 s are depicted in Fig. 17, displaying the wave height, heave and pitch motions and the flap deflection angle. The grey lines indicate the motions of the vessel with active flaps, whereas the black lines present the motions of the vessel without flaps. The pitch angle time trace shows a clear reduction of the positive peaks values using the ride control system. However, the effect on the heave



Fig. 16. Parent hull form DSDS  $25^\circ$ .

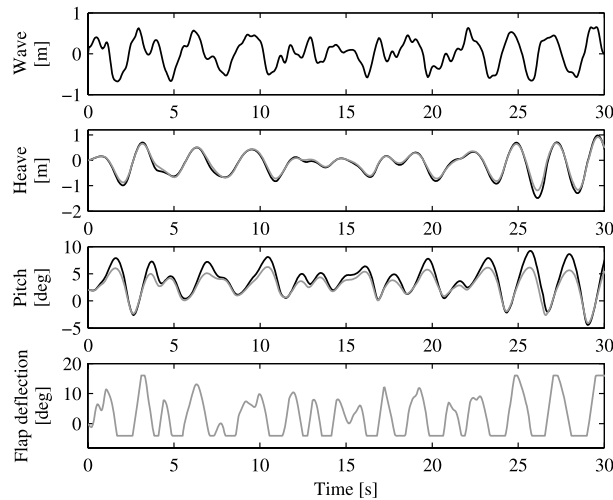


Fig. 17. Time series in irregular waves without transom flaps (black line) and with active transom flaps (grey line).

motion is rather limited. The flaps itself perform a strong oscillatory motion. This behaviour suggests that the forces generated by the active flaps can be frequency dependent. In addition, phase differences may become important between the deflection angle and forces of the flap.

The frequency dependence of the forces generated by oscillating flaps was experimentally investigated by Jurgens et al. [8]. The pitching moment coefficient increases with frequency, mainly caused by a longitudinal translation by the centre of effort of the added lift. This resulted in an increase in efficiency of the transom flap at higher oscillation frequencies. Steen [17] evaluated model tests data of the dynamic response of a harmonic oscillating interceptor performed at the Marine Technology Centre in Trondheim, Norway. He defined a ratio between the average drag force of the oscillating interceptor, relative to the static drag force at maximum amplitude excursion. This ratio was fairly consistent over the different oscillation frequencies considered ranging between 0.7 and 1.0. On the other hand, the ratio between the average dynamic lift and the static lift case at maximum amplitude deflection was found to be very much frequency dependent. Values for this ratio started at 0.5 for low frequencies going up to approximately 2 times the static lift value at intermediate frequencies, before decreasing again to 0.5 for the very high oscillating frequencies. These studies indicate that a strong oscillating transom flap or interceptor can develop substantial dynamic forces. It seems that for both trim mechanisms the efficiency increases, in particular at certain intermediate frequencies. For an accurate model of the ride control system it is necessary to include these unsteady forces.

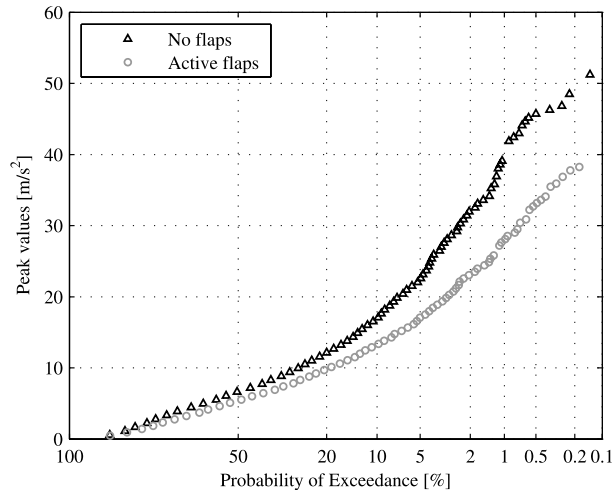


Fig. 18. Distribution of the vertical peak accelerations at the bow without flaps (black markers) and with active flaps (grey markers).

However, the physics and mathematical description of the dynamic behaviour of these trim devices is still far from complete.

A proper procedure to determine the operability of a fast planing vessel has been subject of debate for quite some time. Traditionally, the limiting criteria were based on average or significant values, following the (linear) analysis for displacement vessels. However, for planing vessels this procedure was not applicable due to the strong nonlinear response, in particular for the vertical accelerations. In [11] Keuning concluded that limiting criteria for safe operation on board planing vessels should be based on the actual distribution of the peaks and troughs of the response signals. For optimum operational performance the high amplitude peaks in the vertical acceleration signals with a low frequency of occurrence are the ones to be avoided as much as possible. The distribution curves of the peak values for vertical accelerations at the bow are plotted in Fig. 18 to assess the performance of the ride control system. The difference in the shape of both curves illustrates the improvement in motion behaviour of the vessel. The maximum vertical acceleration level during the one hour trip is reduced by approximately 25%.

## 6. Discussion and further work

In this article trim control is recognized as a valuable method for improving the motion behaviour of fast planing vessels sailing in head waves. Active trim devices can effectively be used to establish a momentarily change in the running trim. This

can result in lower levels of vertical accelerations, which will improve the operability of the vessel.

To better understand the physics of the control surfaces and enable the design for efficient controllers, a mathematical model is extended to include the effects of active control devices. Hydrodynamic characteristics of transom flaps and interceptors are determined with captive model testing. Generally good correlation is found between the experimental results for lift and drag curves compared to the expressions found in literature. Flaps are able to generate negative lift forces at small up angle positions (up to  $-4^\circ$ ), for larger negative angles flow separation causes a sudden drop in the added lift of the flaps. Comparing the lift-to-drag ratio of flaps and interceptors revealed no significant difference in efficiency for steady running conditions, however for a more thorough comparison a larger set of data points at small interceptor excursions would be desirable.

The pitch velocity signal is an effective control parameter for reducing the motions of a planing vessel sailing in regular head waves. Next to a reduction in pitch motions over a broad range of wave lengths also a positive effect in heave motion response is noticed. The comparison between the simulations and the model test data, indicates that the mathematical model yields reasonable results for the prediction of the response characteristics of a planing vessel with active transom flaps. However, the experimental data available to validate simulations is limited and the model tests were carried out in relatively small regular waves. At these conditions small flap deflections already lead to a significant reduction in the motion response. In more severe wave conditions strong oscillatory motions of the control devices can induce frequency dependent forces. This means that the forces added by the control devices may no longer be considered in a quasi-steady manner. Nevertheless, it is thought that the present mathematical model can be used for qualitative analysis to investigate the effects of different control algorithms. In irregular waves pronounced reductions have been found in the extreme peak accelerations at the bow using a pitch velocity feedback control system.

Extending the mathematical model to control roll motions by steering the trim devices on portside and starboard independently is a valuable next step to make the program suited for quartering or beam seas. Furthermore, effort should be placed on investigating the unsteady forces generated with (strong) oscillating control devices. Finally, after extensive validation of the computational results with model experiments, the program can be used to develop advanced ride control systems. Due to the strong nonlinear response of a planing vessel to incoming waves a single control algorithm that is effective for the wide variety of operational conditions may be difficult to derive. For optimal performance sensors need to be developed that can register the actual wave profile in front of the vessel. The wave data can subsequently be used in very fast on board simulation routines to calculate wave impact predictions and find optimal settings for the actuators. These so-called anticipating systems could further improve the seakeeping behaviour of planing vessels and should therefore be exploited.

## References

- [1] D.L. Blount and L.T. Codega, Dynamic stability of planing boats, *Marine Technology* **29**(1) (1992), 4–12.
- [2] P.W. Brown, An experimental and theoretical study of planing surfaces with trim flaps, Technical report SIT-DL-71-1463, Stevens Institute of Technology, Davidson Laboratory, April 1971.
- [3] J. Calix St. Pierre, J.P. Hackett, C. Bigler and F.H.H.A. Quadvlieg, Controllability of high-speed craft, in: *Proceedings of the 10th International Symposium on Practical Design of Ships and Other Floating Structures*, 2007.
- [4] D. Dawson and D.L. Blount, Trim control, *Professional Boatbuilder* **75**(February/March) (2002).
- [5] G. Fridsma, A systematic study of the rough-water performance of planing boats, Technical report 1275, Stevens Institute of Technology, Davidson Laboratory, November 1969.
- [6] G. Fridsma, A systematic study of the rough-water performance of planing boats – Part 2 irregular waves, Technical report, Stevens Institute of Technology, Davidson Laboratory, March 1971.
- [7] A.J. Jurgens and F. van Walree, Hydrodynamic aspects of interest for the development of an integrated ride control system for high speed mono hulls, in: *Proceedings of the 7th International Conference on Fast Sea Transportation*, 2003.
- [8] A.J. Jurgens, F. van Walree, M.X. van Rijsbergen and P. van der Klugt, R&D on an advanced ride control system for a high speed mono hull, in: *Proceedings of the 3rd International EuroConference on High-Performance Marine Vehicles*, Bergen, September 2002, pp. 248–261.
- [9] T. Katayama, K. Suzuki and Y. Ikeda, A new ship motion control system for high-speed craft, in: *Proceedings of the 7th International Conference on Fast Sea Transportation*, 2003.
- [10] J.A. Keuning, The nonlinear behaviour of fast monohulls in head waves, PhD thesis, Delft University of Technology, Ship Hydromechanics Laboratory, 1994.
- [11] J.A. Keuning, “Grinding the bow” or “How to improve the operability of fast monohulls”, *International Shipbuilding Progress* **53**(4) (2006), 281–310.
- [12] A. Millward, Effect of wedges on the performance characteristics of two planing hulls, *Journal of Ship Research* **20**(4) (1976), 224–232.
- [13] M. Santos, R. Lopez and J.M. de la Cruz, Fuzzy control of the vertical acceleration of fast ferries, *Control Engineering Practice* **13** (2005), 305–313.
- [14] D. Savitsky, Hydrodynamic design of planing hulls, *Marine Technology* **1**(1) (1964), 71–95.
- [15] D. Savitsky, On the subject of high-speed monohulls, in: *The Society of Naval Architects & Marine Engineers*, October 2003.
- [16] D. Savitsky and P.W. Brown, Procedures for hydrodynamic evaluation of planing hulls in smooth and rough water, *Marine Technology* **13**(4) (1976), 381–400.
- [17] S. Steen, Experimental investigation of interceptor performance, in: *Proceedings of the 9th International Conference on Fast Sea Transportation*, 2007.
- [18] J.J. van den Bosch, Tests with two planing boat models in waves, Technical report 266, Delft University of Technology, Ship Hydromechanics Laboratory, February 1970.
- [19] P.G.M. van der Klugt, F. van Walree and P.M. Pauw, The HSF-Arcos research project, in: *Proceedings of the 6th Symposium on High Speed Marine Vehicles*, September 2002.
- [20] L.W. Wang, A study on motions of high speed planing boats with controllable flaps in regular waves, *International Shipbuilding Progress* **32**(365) (1985), 6–23.
- [21] H. Xi and J. Sun, Feedback stabilization of high-speed planing vessels by a controllable transom flap, *IEEE Journal of Oceanic Engineering* **31**(2) (2006), 421–431.
- [22] E.E. Zarnick, A nonlinear mathematical model of motions of a planing boat in regular waves, Technical report DTNSRDC-78/032, David W. Taylor Naval Ship Research and Development Center, March 1978.